

Chemical Bonding in Metal-Rich Nitrides of Indium

Martin Kirchner, Andreas Schlechte, Walter Schnelle, Frank R. Wagner, Rüdiger Kniep, and Rainer Niewa¹

The ternary systems $A\text{-In-N}$ ($A = \text{Ca}, \text{Sr}, \text{Ba}$) contain a number of compounds which were characterized during the past 20 years [1-9]. The compounds known thus far may be described based on polyhedra of alkaline-earth metal species, which surround nitride ions, stacked in various arrangements together with indium clusters. In the cationic substructures the polyhedra are found to be isolated, vertex-, and/or edge-sharing. The In arrangements extend from isolated tetrahedra [In_4], trigonal bipyramidal [In_5] clusters, [In_8] ions (2-fold edge-capped octahedron) to infinite chains. The chemical bonding in these compounds is inconsistent with simple electron counting rules – accordingly, they are expected to exhibit metallic properties. However, there are open questions according to the exact compositions of certain phases, which would have a profound impact on the interpretation of the chemical, physical and bonding properties. In an explorative project we studied these systems in detail to discover new compounds, unravel the question of exact compositions and study the basic electronic properties. These data, together with electronic structure calculations enable us to get a deeper view in chemical bonding principles in such metal-rich compounds.

$(A_4\text{N})[\text{In}_2]$ ($A = \text{Ca}, \text{Sr}$)

The crystal structures of $(A_4\text{N})[\text{In}_2]$ ($A = \text{Ca}, \text{Sr}$) contain alternating layers of parallel zigzag chains of In and perovskite type layers (respective layers corresponding to ${}^2_2[\text{NiF}_4^{2-}]$ of the $\text{K}_2[\text{NiF}_4]$ type) of corner-sharing octahedra ($A_2A_{4/2}\text{N}$) (Fig. 1). The stacking sequence of ($A_2A_{4/2}\text{N}$) layers corresponds to ...**ABCD**..., while the layers in the $\text{K}_2[\text{NiF}_4]$ type are arranged according to ...**AB**.... This different arrangement results from the formation of [In] zigzag chains (distance $d(\text{In-In}) = 316.3$ pm) indicating some homoatomic bonding attraction of In. These zigzag chains of In would indicate a description with two-bonded homoatomic bonds ${}^1_\infty[\text{In}^{3-}]$ according to the Zintl-rule, which is inconsistent with the ionic formula $(A^{2+})_4(\text{N}^{3-})[(\text{In}^{2.5-})_2]$. The

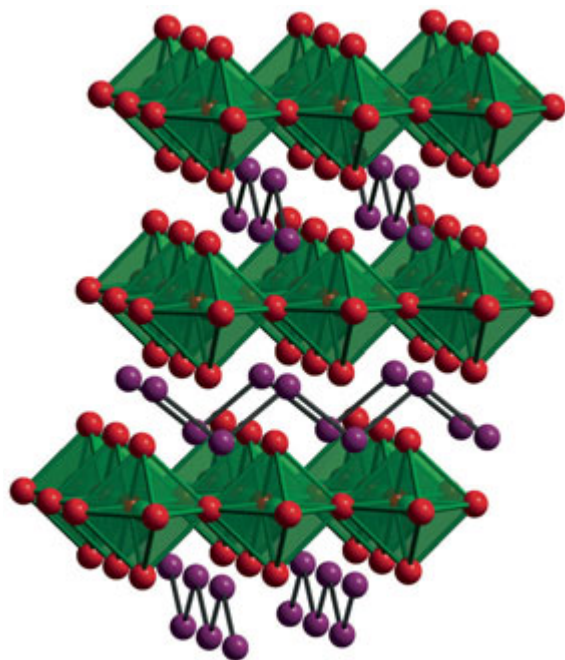


Fig. 1: Section of the crystal structure of $(\text{Ca}_4\text{N})[\text{In}_2]$: Slabs of vertex-sharing octahedra ($\text{Ca}_2\text{Ca}_{4/2}\text{N}$) (green) alternating with layers of parallel orientated [In] zigzag chains (violet spheres).

comparison of the interchain distance with e. g. $d(\text{In-In}) = 294.1$ pm in LiIn with the NaTl structure type [10] reveals the distance in the nitride to be rather long. It is therefore not surprising that the formulation with a Zintl ion does not hold. Chemical analyses on samples of $(\text{Ca}_4\text{N})[\text{In}_2]$ showed no significant contamination with oxygen. This rules out an alternative interpretation as $(\text{Ca}_4\text{O})[\text{In}_2]$, which would be in accordance with ionic counting. On going from $(\text{Ca}_4\text{N})[\text{In}_2]$ to the isotype $(\text{Sr}_4\text{N})[\text{In}_2]$ the already comparatively long intrachain distance In-In in $(\text{Ca}_4\text{N})[\text{In}_2]$ further increases substantially (Ca: $d(\text{In-In}) = 316.3$ pm, Sr: $d(\text{In-In}) = 331.8$ pm) accompanied by a marked increase of the interchain distances within the layers of zigzag chains from $d(\text{In-In}) = 491.5$ pm to $d(\text{In-In}) = 524.0$ pm, respectively. These distances are largely determined by the $A\text{-N}$ distances in the quite rigid ${}^2_2(A_2A_{4/2}\text{N})$ slabs: The interchain distance

equals the distance between two opposite lateral edges of (A_6N) octahedra ($2 \times d(A-N)$), and the projection of the intrachain distances into the lateral $\frac{2}{\infty}(A_2A_{4/2}N)$ plane equals the distance $d(A-N)$. Due to these geometric constraints, the increase of the interchain distances is approximately twice the increase of the intrachain distance on going from $(Ca_4N)[In_2]$ to $(Sr_4N)[In_2]$ for a nearly constant intrachain angle (about 103°). Apparently, in these phases the intrachain In–In interactions are less important than a picture with strong covalent bonds would suggest. The result is a three-dimensional structure with competing interactions In–In, A –In and A –N as evidenced and discussed in deeper detail with electronic structure calculation results below.

Measurements of the magnetic susceptibility on $(Ca_4N)[In_2]$ reveal diamagnetic behavior. Fig. 2 depicts the temperature dependence of the magnetic susceptibility and the electrical resistivity. A fit of a modified Curie-law to the magnetic susceptibility (extrapolated to $1/H \rightarrow 0$) resulted in a temperature independent magnetic susceptibility $\psi_0 = -20(5) \times 10^{-6}$ emu/mol. Subtraction of diamagnetic ion core corrections ($Ca^{2+} + In^{3+} + N^{3-}$ [11, 12]) yields a small Pauli-paramagnetic contribution ($\chi_0 - \chi_{core}$) $\approx +62 \times 10^{-6}$ emu/mol consistent with a metallic state with a low density of states DOS at the Fermi level E_F ($DOS(E_F)_{max} \approx 1.9$ states/eV per 2 spin directions). The temperature dependence of the electrical resistivity r and the residual resistivity of $\rho_0 \approx 350 \mu\Omega$ cm as well as the resistivity

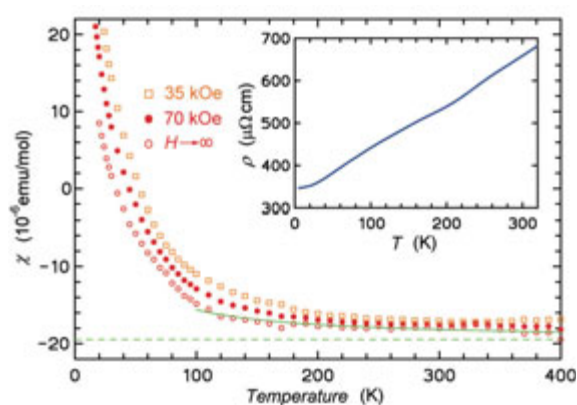


Fig. 2: Magnetic susceptibility of $(Ca_4N)[In_2]$ measured in external fields of $H = 35$ kOe (upper open orange data) and $H = 70$ kOe (middle solid red data), extrapolation to $1/H \rightarrow 0$ (lower open violet data and fitted solid green line), resulting temperature independent susceptibility (dashed green line) and electrical resistivity (inset, blue line) as a function of temperature.

at ambient temperature of about $680 \mu\Omega$ cm are consistent with the description as a bad metal, in agreement with the composition as discussed above and the chemical bonding on which we are going to focus on below.

$(A_{19}N_7)[In_4]_2$ ($A = Ca, Sr$)

$(Ca_{19}N_7)[In_4]_2$ was first reported with the composition $(Ca_{18.5}N_7)[In_4]_2$ (together with the isotype $(Ca_{18.5}N_7)[Ga_4]_2$) [2], but only metric information and space group were communicated together with a brief description of the crystal structure. The difference in composition supposedly originates in Zintl-type ionic counting according to $(Ca^{2+})_{18.5}(N^{3-})_7([In_4]^{8-})_2$ containing $[In_4]$ tetrahedra with three-bonded In^{2-} species. From experimental data the decision between the two compositions is very difficult. However, Rietveld refinements on the basis of X-ray and neutron powder diffraction data gave no evidence for any Ca deficiency and the chemical analyses also indicate full occupancy for all atomic positions ($(Ca_{19.0(2)}N_{6.87(9)})[In_{7.954(7)}]$). No sufficient carbon or hydrogen impurities were detected, which could resolve the electronic imbalance resulting from a simple Zintl-type counting $(Ca^{2+})_{19}(N^{3-})_7([In_4]^{8-})_2 \cdot e^-$ due to substitution of N^{3-} by C^{4-} or additional occupation of interstitial sites by H^- . A partial substitution of Ca by Na or K was also excluded. Similar observations were made for the Sr containing isotype. The crystal structure of the isotype $(Ca_{19}N_7)[Ag_4]_2$ was refined earlier on the basis of single crystal X-ray diffraction data [13].

For an electronically balanced compound in the sense of the Zintl-concept with the composition $(Ca_{18.5}N_7)[In_4]_2 = (Ca^{2+})_{18.5}(N^{3-})_7([In_4]^{8-})_2$ one might expect semiconducting behavior while $(Ca_{19}N_7)[In_4]_2$ should be metallic. However, electronic structures with a pseudo-minimum at the Fermi energy E_F were frequently found for Zintl-phases with $E =$ group 13 elements which obey the Zintl-rule and compounds with electronic situations close to Zintl-phases. Fig. 3 depicts the magnetic susceptibility and the electrical resistivity of $(Ca_{19}N_7)[In_4]_2$. The compound shows diamagnetic behavior with $\chi_0 = -190(40) \times 10^{-6}$ emu/mol. For $(Sr_{19}N_7)[In_4]_2$ we find $\chi_0 = -230(30) \times 10^{-6}$ emu/mol. Subtraction of the diamagnetic ion core corrections result in Pauli-paramagnetism $(\chi_0 - \chi_{core}) = +198(40) \times 10^{-6}$ emu/mol and $(\chi_0 - \chi_{core}) =$

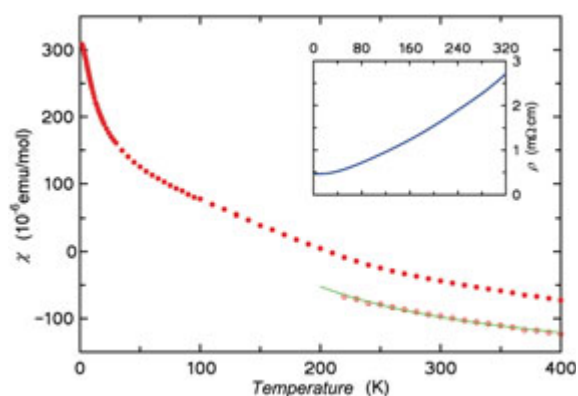


Fig. 3: Magnetic susceptibility of $(Ca_{19}N_7)[In_4]_2$ measured in external fields of $H = 70$ kOe (upper red data) and extrapolation to $1/H \rightarrow 0$ (lower red data and fitted green line), and electrical resistivity (inset, blue line) as function of temperature.

$+290(30) \times 10^{-6}$ emu/mol for the Ca and Sr containing compounds. These values correspond to maximum electronic density of states of $D(E_F)_{\max} \approx 6.1$ states/eV and $D(E_F)_{\max} \approx 9.0$ states/eV (per 2 spin directions). The temperature dependence of the electrical resistivity ρ and the residual resistivity ρ_0 of the order of only few $\mu\Omega$ cm are consistent with heavily doped semiconductors as well as metallic states with very low concentrations of conduction electrons.

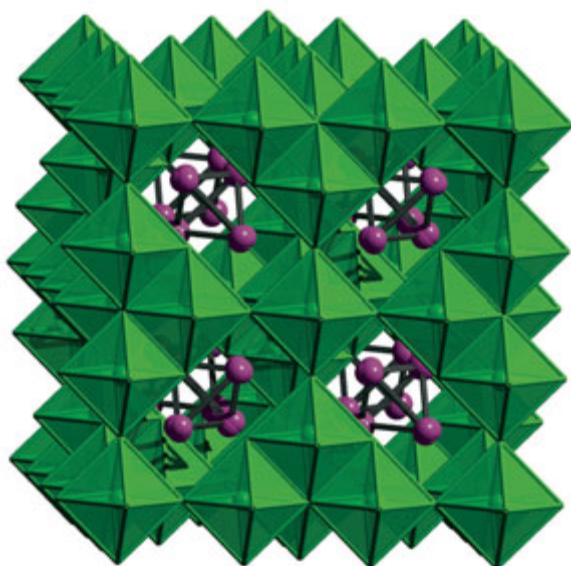


Fig. 4: Crystal structure of $(A_{19}N_7)[In_4]_2$: $[In_4]$ tetrahedra (In: violet spheres) embedded in a framework of edge- and corner-sharing (A_6N) octahedra (green).

The crystal structure of the isotypes $(A_{19}N_7)[In_4]_2$ ($A = Ca, Sr$) consists of an open framework of edge- and vertex-sharing octahedra (A_6N) in which regular $[In_4]$ tetrahedra are embedded (Fig. 4). The environment of In is completed by nine nearest alkaline-earth metal neighbors. In the cationic framework six octahedra share common edges and one central A to form $(A_{19}N_6)$ “superoctahedra”, which are connected at the six terminal A vertices via further N^{3-} in octahedral coordination (Fig. 5a). This way of linking leads to the three-dimensional framework. Similar “superoctahedra” are known, e. g., from oxometalates containing isolated complex ions $[M_6O_{19}]$ ($M = Nb, Ta, Mo, W$) [14], however,

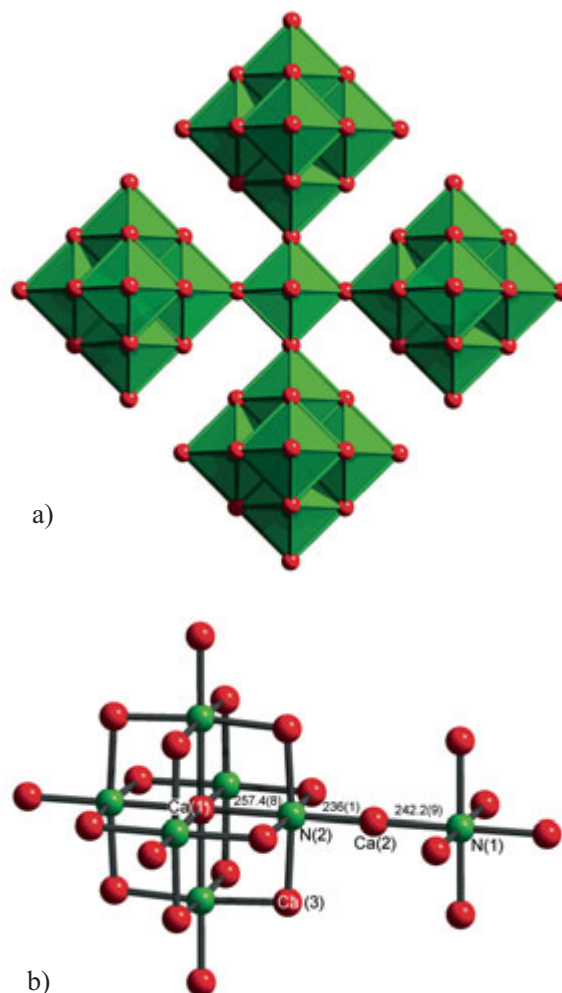


Fig. 5: Sections of the crystal structure of $(A_{19}N_7)[In_4]_2$: a) $(A_{19}N_6)$ “superoctahedra” of six edge- and vertex-sharing (A_6N) octahedra (green) surrounding one central A^{2+} ion linked three-dimensionally via further (A_6N) octahedra. b) $(A_{19}N_6)$ “superoctahedron” (A : red spheres, N : green spheres) linked to an (A_6N) octahedron, distances in pm for $(Ca_{19}N_7)[In_4]_2$.

with an inverse occupation compared to the ternary nitrides under discussion. A remarkable feature of both the $[M_6O_{19}]$ ions as well as the $(A_{19}N_6)$ building units is their distortion (Fig. 5b): In $(Ca_{19}N_7)[In_4]_2$ the distance of N(2) to the central Ca(1) of the superoctahedron is enlarged to $d(N(2)-Ca(1)) = 257.4(8)$ pm and the opposite distance shortened to $d(N(2)-Ca(2)) = 236(1)$ pm. All distances in $(Ca_{19}N_7)[In_4]_2$ are similar to the respective distances found for the isotype $(Ca_{19}N_7)[Ag_4]_2$. The Ca–N distances are in the range of those in, e.g., Ca_2N with $d(Ca-N) = 244.26(4)$ pm and N in octahedral coordination [15]. An isostructural compound $(K_{19}O_4(OH)_3)[Pb_4]_2$ which obeys the $(8 - N)$ rule was previously described [16]. The $[In_4]$ tetrahedra with distances of $d(In-In) = 311.6(3)$ pm ($A = Ca$) and $d(In-In) = 309.7(3)$ pm ($A = Sr$) are similar to those in, e.g., $Na_2In \equiv Na_8[In_4]$ containing distorted tetrahedra $[In_4]^{8-}$ (according to the Zintl concept) with $d(In-In) = 307$ pm – 315 pm [17].

$(Ba_6N)[In_5]$

$(Ba_6N)[In_5]$ is an isotype of $(A_6N)[Ga_5]$ ($A = Sr, Ba$) [18]. The crystal structure of $(Ba_6N)[In_5]$ is characterized as rocksalt type motif of N-centred octahedra (Ba_6N) and trigonal bipyramidal clusters $[In_5]$ (Fig. 6). The trigonal bipyramidal $[In_5]$ units might be described as $[In_5]^{7-}$ ions according to the Wade-rules for closo-clusters. The isotopes $(A_6N)[Ga_5]$ ($A = Sr, Ba$) were previously described by the formula $(A^{2+})_6(N^{3-})[Ga_5]^{7-} \cdot 2e^-$ based on electronic structure calculations. An alternate speculation on unnoticed hydride ion impurities in the sense of ‘ $(A_6N)[E_5]H_2$ ’ ($E = Ga, In$) was laid to rest by chemical analyses of hydrogen on a nearly single phase sample. For comparison, for the $[In_5]$ cluster in $(Ba_{38}N_{18})[In_5]_2[In_8]$ a highly electron deficient situation ($[In_5]^{5-}$) was derived [4]. Distances within the $[In_5]$ unit in $(Ba_6N)[In_5]$ with $d(In-In)_{equatorial} = 306.1(1)$ pm and $d(In-In)_{axial} = 305.7(1)$ pm are in the range of the respective distances in $(Ba_{38}N_{18})[In_5]_2[In_8]$ with $d(In-In)_{equatorial} = 311.5(1)$ pm, 316.4(1) pm and $d(In-In)_{axial} = 295.5(1)$ pm – 322.4(2) pm. The distances in the isolated (Ba_6N) octahedra with $d(Ba-N) = 278.27(8)$ pm are similar to those in $(Ba_6N)[Ga_5]$ ($d(Ba-N) = 273.4(1)$ pm).

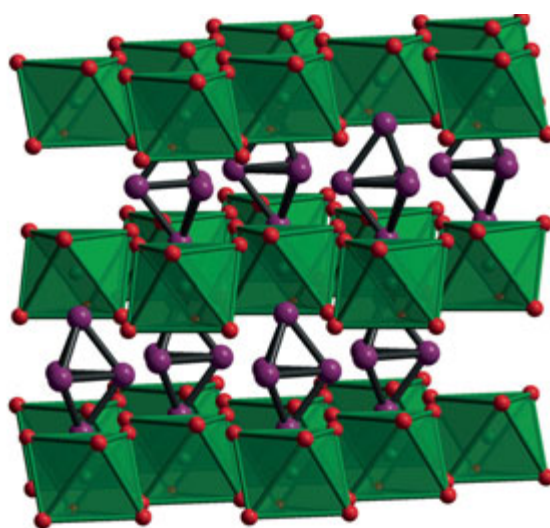


Fig. 6: Section of the crystal structure of $(Ba_6N)[In_5]$: Arrangement of $[In_5]$ trigonal bipyramidal clusters (violet spheres) and (Ba_6N) octahedra (green).

Electronic Situations

The calculated DOS for $(Ca_4N)[In_2]$ exhibits a pseudo-gap in the Fermi level region with 2 states/eV at the local minimum (Fig. 7a). Noteworthy, the DOS for $(Ca_{19}N_7)[In_4]_2$ even displays a small “band gap” of about 0.05 eV in the region close to E_F (Fig. 8a). The local minima of the DOS close to E_F correspond to the respective Zintl-type electron count, which is one indication that the electronic structures of both compounds are still related to those expected for Zintl compounds. The Fermi level of $(Ca_4N)[In_2]$ lies just at the sloping flank below $E(DOS_{min})$, the Fermi level of $(Ca_{19}N_7)[In_4]_2$ at the rising flank above $E(DOS_{min})$. The calculated densities of states at E_F are 5 states/eV and 8 states/eV for $(Ca_4N)[In_2]$ and $(Ca_{19}N_7)[In_4]_2$, respectively, in reasonable agreement with the values from magnetic susceptibility measurements (see above).

As pointed out above a purely ionic electron counting for $(Ca_4N)[In_2]$ arrives at $(Ca^{2+})_4(N^{3-})[(In^{2.5-})_2]$, which is not consistent with a Zintl-type electron counting requiring In^{3-} species with homonuclear bonds within the zigzag chains. Accordingly, the In species would be electron deficient. On the basis of extended Hückel theory calculations a more adequate description according to $(Ca^{1.75+})_4(N^{3-})[(In^{2-})_2]$ or

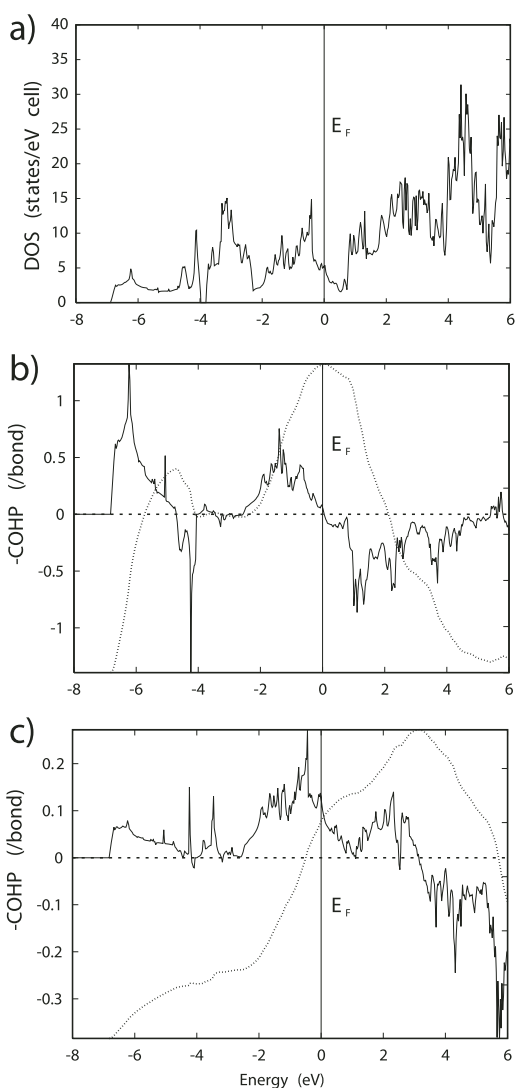


Fig. 7: Electronic structure of $(Ca_4N)[In_2]$. a) Total DOS, b) and c) COHP(E) diagrams for orbital interactions per bond b) In–In and c) In–Ca(2) (exemplarily for In–Ca). Integrated COHP (ICOHP(E)) curves are shown as dotted lines.

$(Ca^{2+})_4(N^{3-})[(In^{2-})_2](e^-)$ has been suggested [19]. It was found from In–In crystal orbital overlap population (COOP) curves that the bonding orbital interactions between nearest neighbors within the chains are completely exhausted up to the Fermi level. This finding is supported by our crystal orbital Hamiltonian population (COHP) analysis (Figs. 7b, c). Concerning the chemical interpretation of the electronic structure we come to a slightly different interpretation. According to the $(8 - N)$ rule additional electrons beyond a valence electron concentration (VEC) of 4 lead to a reduced bond

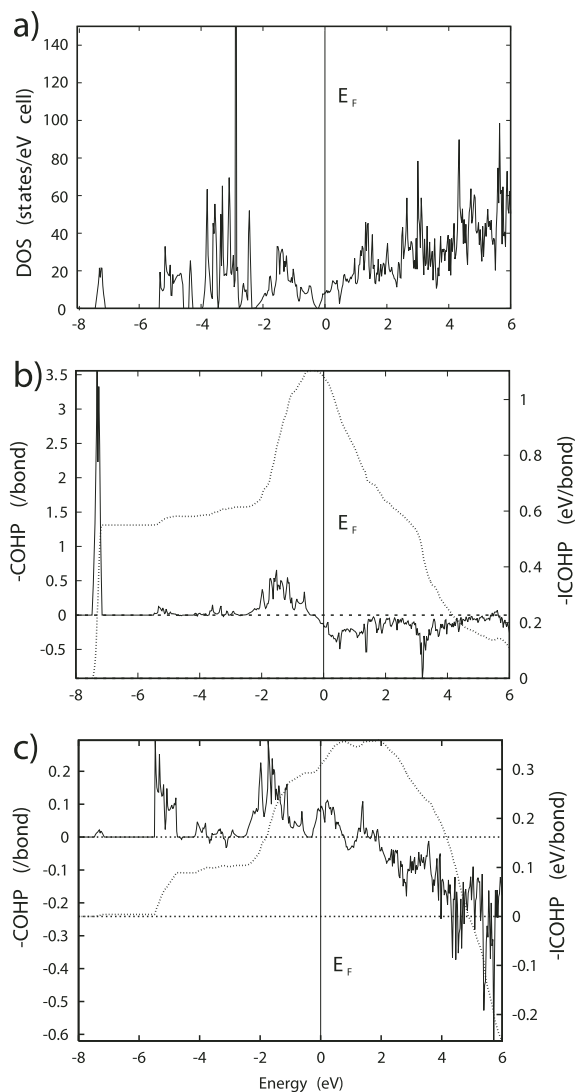


Fig. 8: Electronic structure of $(Ca_{19}N_7)[In_4]$. a) Total DOS, b) and c) COHP(E) diagrams for orbital interactions per bond b) In–In and c) In–Ca(2) (exemplarily for In–Ca). Integrated COHP (ICOHP(E)) curves are shown as dotted lines.

order and the formation of lone pairs instead. The question arises whether the decreased VEC of In of slightly below 6 causes either an increase of homoatomic bonding along the chain (i. e., π -bonding) or the partial destruction of at least one of the formally two lone pairs of two-bonded In^{3-} . Already from the distance $d(In-In)$ an increase of In–In bond order can be regarded as unlikely. Inspection of the band structure shows that those bands containing the π -type p -orbitals are crossing E_F and remain partially unfilled, while they should be completely filled for two-bonded In^{3-} . As these

bands are effectively π -nonbonding they must be interpreted as unsaturated lone pairs, which find their interaction partners elsewhere. Of course, surrounding Ca atoms are available as bonding partners, and COHP diagrams prove significant In–Ca bonding orbital interactions. However, these interactions do not benefit from the reduced electronic population of the In atoms, since the significant bonding interaction is increasing further beyond E_F . In this respect the situation resembles the one discussed for Tl–Ca bonding in $(\text{Ca}_3\text{N})\text{Tl}$ [20].

There is no indication from the band structure that the formal Ca^{2+} cations are significantly electronically populated in order to account for an — in the Zintl-sense — unsaturated In species. We do not expect the Ca species of $(\text{Ca}_4\text{N})[\text{In}_2]$ to be significantly different from those in the hypothetical isostructural compound “ $(\text{Ca}_4\text{O})[\text{In}_2]$ ”, which would formally obey Zintl’s rule. Therefore, we prefer the initial ionic notation $(\text{Ca}^{2+})_4(\text{N}^{3-})[(\text{In}^{2.5-})_2]$ for the conceptual description of the electronic structure.

A purely ionic counting for $(\text{Ca}_{19}\text{N}_7)[\text{In}_4]_2$ arrives at $(\text{Ca}^{2+})_{19}(\text{N}^{3-})_7[(\text{In}^{2.125-})_4]_2$ which is not consistent with a Zintl-type electron counting requiring In^{2-} species with three homonuclear bonds for $[\text{In}_4]$ tetrahedra. According to this approach, In species end up with an electron excess. The analysis of DOS and COHP diagrams supports the interpretation that the one excess electron per formula unit occupies In majority states. Thus, conceptually each $[\text{In}_4]$ tetrahedron contains $\frac{1}{2}$ electron in excess, which occupies In–In antibonding states (Fig. 8b). For the breaking of one of the 2-center bonds 2 electrons would be necessary – much more than are available. The observed fractional occupation of antibonding states rather decreases the In–In bond order, but simultaneously increases the occupation of In lone pair type states. These states are outwardly directed from the tetrahedron, where the contacts In–Ca are located. Therefore, the excess electron leads to an increased occupation of In–Ca bonding states (represented by $\text{ICOHP}(\text{In–Ca})$), which appears to compensate for the loss of covalent homoatomic interaction ($\text{ICOHP}(\text{In–In})$, see Figs. 8b, c). Although the orbital interactions In–In (per bond) are clearly

stronger than In–Ca, the latter can, nevertheless, collectively compete due to their larger number: each In atom has 3 homoatomic neighbors but 9 Ca neighbors. Similar to what was discussed for $(\text{Ca}_4\text{N})[\text{In}_2]$ there is no indication from the band structure analysis for a significant occupation of the formal Ca^{2+} states.

Considering both Ca containing compounds, $(\text{Ca}_4\text{N})[\text{In}_2]$ and $(\text{Ca}_{19}\text{N}_7)[\text{In}_4]_2$, which electronically represent examples for slight deviations from the $(8 - N)$ rule, the question arises about the prerequisites of a system to favor this kind of situations. Some arguments can be put forward: Homoatomic bonding should be comparatively weak, so that bonding interactions with other constituents can compete. The competing constituents should be metals of small electronegativity from the left of the Zintl border, the number for these heteroatomic interactions being preferably larger than the homoatomic. A stable cationic partial structure $((\text{Ca}_{19}\text{N}_7); (\text{Ca}_4\text{N}))$, which acts as a confining matrix for the In partial structure and small electronegativity differences and/or high formal charge transfer between the metal and the Zintl species should be present.

Conclusion

In conclusion, the ternary nitrides $(A_{19}\text{N}_7)[\text{In}_4]_2$ ($A = \text{Ca}, \text{Sr}$) and $(\text{Ca}_4\text{N})[\text{In}_2]$ violate classical electronic counting rules by electron excess or deficiency, respectively. Electronic structure calculations on the Ca containing representatives $(\text{Ca}_{19}\text{N}_7)[\text{In}_4]_2$ and $(\text{Ca}_4\text{N})[\text{In}_2]$ reveal heteroatomic Ca–In bonding to overcompensate the electronic imbalance – a situation which may be expected for phases with comparatively small electronegativity differences of the metallic constituents, large numbers of heteroatomic contacts of the Zintl-metal atoms and high formal charge transfer to the metal with the higher electronegativity. This indicates that for such compounds of the group 13 element indium the Zintl-type counting does not strictly apply; homoatomic In–In interactions are less dominant compared to homoatomic bonding in classical Zintl-phases.

References

- [1] *M. Kirchner, W. Schnelle, F. R. Wagner, R. Kniep and R. Niewa*, *Z. Anorg. Allg. Chem.* **631** (2005) 1477.
- [2] *G. Cordier and S. Rönninger*, *Z. Kristallogr. Suppl.* **182** (1988) 60.
- [3] *A. Schlechte, Yu. Prots and R. Niewa*, *Z. Kristallogr. NCS* **219** (2004) 349.
- [4] *H. Yamane, S. Sasaki, T. Kajiwara, T. Yamada and M. Shimada*, *Acta Crystallogr. E* **60** (2004) i120.
- [5] *P. Höhn, R. Ramlau, H. Rosner, W. Schnelle and R. Kniep*, *Z. Anorg. Allg. Chem.* **630** (2004) 1704.
- [6] *M. Ludwig*, Ph. D. Thesis, TU Darmstadt, Germany, 1998.
- [7] *P. Höhn, R. Ramlau, H. Rosner, W. Schnelle and R. Kniep*, contribution within this Scientific Report.
- [8] *M. S. Bailey and F. J. DiSalvo*, *J. Alloys Comp.* **353** (2003) 146.
- [9] *G. Cordier and S. Rönninger*, *Z. Naturforsch.* **42b** (1987) 825.
- [10] *W. A. Alexander, L. D. Calvert, R. H. Gamble and K. Schinzel*, *Can. J. Chem.* **54** (1976) 1052.
- [11] *P. W. Selwood*: *Magnetochemistry*, Interscience, New York, 2nd Ed., 1956.
- [12] *S. Leoni, R. Niewa, L. Akselrud, Yu. Prots, W. Schnelle, T. Göksu, M. Cetinkol, M. Somer and R. Kniep*, *Z. Anorg. Allg. Chem.* **631** (2005) 1818.
- [13] *O. Reckeweg, T. P. Braun, F. J. DiSalvo and H.-J. Meyer*, *Z. Anorg. Allg. Chem.* **626** (2000) 62.
- [14] *F. Pickhar and H. Hartl*, *Z. Anorg. Allg. Chem.* **623** (1997) 1311 and references given herein.
- [15] *D. H. Gregory, A. Bowman, C. F. Baker and D. P. Weston*, *J. Mater. Chem.* **10** (2000) 1635.
- [16] *C. Röhr*, *Z. Naturforsch.* **50b** (1995) 802.
- [17] *S. C. Sevov and J. C. Corbett*, *J. Solid State Chem.* **103** (1993) 114.
- [18] *G. Cordier, M. Ludwig, D. Stahl, P. C. Schmidt and R. Kniep*, *Angew. Chem.* **107** (1995) 1879.
- [19] *G. J. Miller*, in: *Chemistry, Structure, and Bonding of Zintl Phases and Ions*, S. M. Kauzlarich (Ed.), VCH, Weinheim, 1996, p. 35.
- [20] *R. Niewa, W. Schnelle and F. R. Wagner*, *Z. Anorg. Allg. Chem.* **627** (2001) 365.

¹ Present address: TU München, München, Germany